ISSN 2347-3487
Volume 13 Number 3
Journal of Advances in Physics

Structural, Dielectric and Electrical Characteristic of $Bi_{0.5}Pb_{0.5}[Fe_{0.1}La_{0.4}(Zr_{0.25}Ti_{0.25})]O_3$

Niranjan Panda[1*], Samita Pattanayak[2], R.N.P. Choudhary[3], Ashok Kumar[4]
[*1]Department of Physics, DRIEMS,Cuttack, Odissa, India
[2]Department of Physics, CET, Bhubaneswar, Odissa, India
[3]Department of Physics, ITER, Bhubaneswar, Odissa, India
[4]National Physical Laboratory (CSIR), New Delhi, India
*E-mail: niranjan.panda@driems.ac.in

ABSTRACT

The polycrystalline compound $Bi_{0.5}Pb_{0.5}$ $[Fe_{0.1}La_{0.4}$ $(Zr_{0.25}Ti_{0.25})]O_3$ was synthesized by substituting Pb, La, Zr and Ti ions on perovskite structured bismuth ferrite (BFO) with the help of mixed oxide solid state reaction method. The present work is to observe the effect of off-valence and iso-valence substitution on the dielectric and electric properties of bismuth ferrite (BFO). The room temperature XRD pattern of the calcinated powders of the sample reveals that the crystal structure is tetragonal with space group P4mm, while BFO has rhombohedral structure with space group R3c. The SEM of the sintered pellet of the compound indicates that the small grains are uniformly distributed over the surface. Complex impedance spectroscopy (CIS) was adopted to analyze the dielectric, impedance and conductivity behavior of the compound. The results show that the dielectric loss in the material is significantly less than that of BFO and the dielectric and ferroelectric behavior of the sample get enhanced. The complex impedance plots show the existence of non-Debye type of relaxation phenomena, which is caused by resistive and capacitive effect of the bulk and grain boundaries. The Arrhenius plot for the compound indicates that the material possesses NTCR behavior. The frequency response of ac conductivity obeys Jonscher's law and UDR (universal dielectric response).

Key words

off-valence, iso-valence, CIS, non-Debye type relaxation, NTCR, UDR]

1. INTRODUCTION:

The ABO_3 type perovskite material draws the attention of many researchers in the last few decades owing to their unique characteristics suitable for various technological applications [1-4]. The perovskite structured compounds possesses multifunctional properties like ferroelectricity, ferrimagnetism, piezoelectricity and magneto-electric coupling etc. Some of these materials also exhibit more than one ferroic properties simultaneously. In these materials, an applied electric field can induce electrical polarization and a magnetic ordering and an applied magnetic field can induce magnetization and electrical polarization. Due to these specialties, this type of materials finds their application in higher solid-state transformers, multifunctional smart devices, multi-state non volatile memories etc. [5, 6]. Among the perovskite materials bismuth ferrite (BFO) emerged as a promising potential candidate for device applications in the recent years due to its ferroelectric and anti-ferromagnetic state in the same phase [7-9]. Below its ferroelectric transition temperature ($\approx 1103\mathrm{K}$), the perovskite structured $BiFeO_3$ has rhombohedral symmetry with pace group R3c. In BFO, polarization arises mostly from the lone pair (S^2 orbital) of Bi^{3+} ion, while weak magnetism results from Fe^{3+} ion [10].

2. EXPERIMENTAL:

The polycrystalline ceramic compound $Bi_{0.5}Pb_{0.5}$ $[Fe_{0.1}La_{0.4}$ $(Zr_{0.25}Ti_{0.25})]$ O_3 was prepared by a high temperature mixed oxide method using highly pure ingredients; Bi_2O_3 (FINAR-extra pure 99%), and Fe_2O_3, PbO, TiO_2, ZrO_2, La_2O_3 (all are from LOBA CHEME-99.9%) were used as ingredient materials. The stoichiometric proportions of these ingredients are thoroughly mixed and grinded to fine powder in dry (air) for 2h by using agate mortar and pestle. To enhance the homogeneity, the powder sample was again grinded in wet atmosphere (methanol) for 2h. This homogeneously mixed powder of the sample is calcinated at an optimized temperature of 850^{o}C after several trials for 4h in pure alumina crucible. The powder X-ray diffraction method was adopted to check the formation of compound and to analyze the crystal structure by using powder diffractometer (Rigaku Mini flex, Japan). The XRD pattern and data were obtain by using Copper-k_α radiation ($\lambda = 1.5405\mathrm{A}^\circ$) in a Bragg angle range ($20^\circ \leq 2\theta \leq 80^\circ$) at a scanning rate of $3^\circ/\mathrm{min}$ at room temperature. The calcinated powder of the sample was cold pressed using the binder polyvinyl alcohol (PVA) into small circular pellets of approximate thickness 0.1-0.2cm and diameter 1cm with the help of a uni-axial hydraulic press. The circular pellets were sintered for 4hr at an optimized temperature of 900^{o}C. The microstructure of the sample after sintering was recorded at a magnification of 6000k by using scanning electron microscope (SEM JEOL JSM-6510) at room temperature. The parallel flat areas of circular pellets of the sample were properly polished and electroded by using silver paint so that the prepared material can act as a dielectric separation of a parallel plate capacitor. To avoid moisture the pellets were dried at temperature of 150^{o}C for 2hr before it is used to take measurement of its electrical parameters. The values of the electrical parameters such as phase, dielectric loss, impedance, parallel L, parallel C, parallel R ,of the material were recorded in the frequency range of (10^3Hz – 10^6Hz) at temperatures between 25^{o}C to 500^{o}C in the intervals of 5^{o}C with the help of a phase sensitive LCR meter (PSM 1735 N4L). Ferroelectric hysteresis curves were traced at room temperature by using a P~E loop tracer (M/S Radiant Technologies inc. USA) after proper polling of the sintered pellet of the sample.

3. INTERPRETATION OF EXPERIMENTAL RESULTS:

3.1. Structural Analysis :

The X-ray diffraction pattern of the calcinated powder of $Bi_{0.5}Pb_{0.5}$ $[Fe_{0.1}La_{0.4}$ $(Zr_{0.25}Ti_{0.25})]$ O_3 compound is shown in Figure 1. All the XRD peaks were indexed first in various crystal systems (i.e. cubic, rhombohedral, orthogonal and tetragonal) with the help of a reliable computer software 'POWDMULT' [11]. The comparison of the observed value and calculated value shows that both the values are very close to each other in the tetragonal crystal system with space group P4mm. Thus the lattice parameters of the compound were found to be as: $a = 5.5826$, $c = 14.9724$Å, $^c/_a = 2.6820$ and volume = 466.66Å^3. The Goldschimdt's tolerance factor $[(t) = \frac{R_A+R_O}{\sqrt{2}\,(R_B+R_O)}]$ of the compound was found to be 0.836 [12, 13], indicating that in the ABO_3- type perovskite compound $Bi_{0.5}Pb_{0.5}$ $[Fe_{0.1}La_{0.4}$ $(Zr_{0.25}Ti_{0.25})]O_3$, the length of B-O bond is significantly larger than the length of A-O bond. The SEM micrograph of the pellet of the compound recorded at room temperature is shown in Figure-2. It gives a clear signature of the homogeneous distribution of grains over the surface with less porosity.

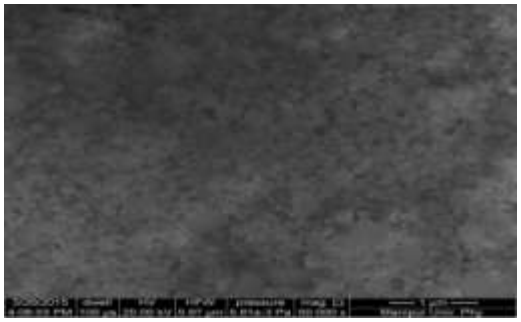

Figure 1: XRD pattern of $Bi_{0.5}$ $Pb_{0.5}$ $[Fe_{0.1}$ $La_{0.4}(Zr_{0.25}Ti_{0.25})]O_3$ compound at room temperature

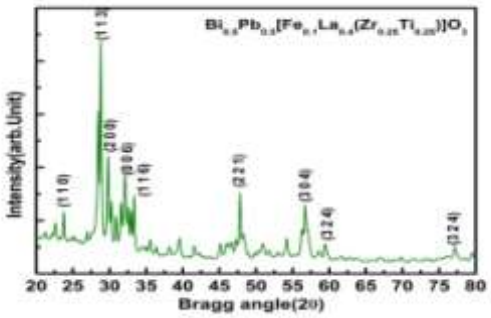

Figure 2: Scanning Electron Micrograph of $Bi_{0.5}Pb_{0.5}$ $[Fe_{0.1}La_{0.4}(Zr_{0.25}Ti_{0.25})]$ O_3 compound at room temperature

3.2. Dielectric Properties:

Figure 3(a -b) shows the variation of the relative permittivity (ε_r) and tangent loss (tanδ) of the compound $Bi_{0.5}Pb_{0.5}$ $[Fe_{0.1}La_{0.4}$ $(Zr_{0.25}Ti_{0.25})]O_3$ with the frequency of the applied electric field at various temperatures in the high-temperature range $300℃ - 400℃$.

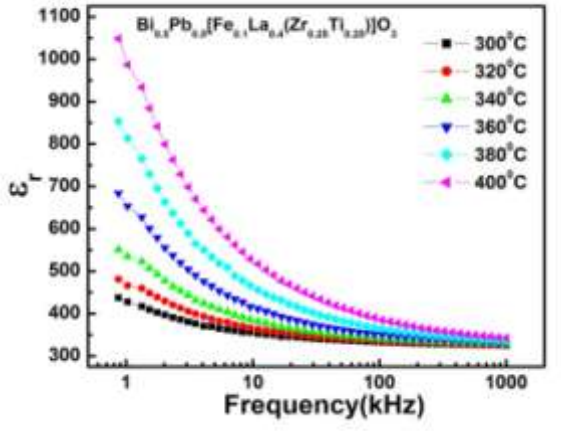

Figure 3(a): Variation of dielectric constant (ε_r) of $Bi_{0.5}Pb_{0.5}$ $[Fe_{0.1}La_{0.4}$ $(Zr_{0.25}Ti_{0.25})]$ O_3 compound with frequency at selected temperatures .

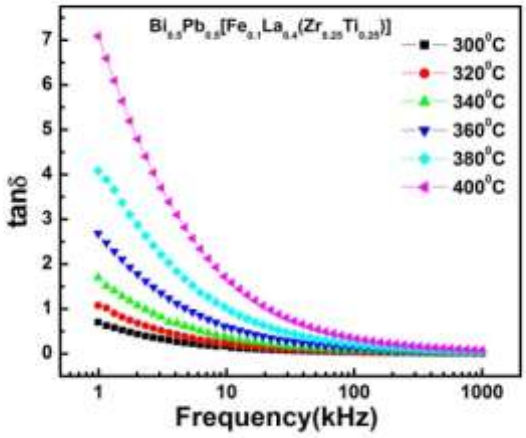

Figure 3(b): Variation of tangent loss ($tan\delta$) of $Bi_{0.5}Pb_{0.5}$ $[Fe_{0.1}La_{0.4}$ $(Zr_{0.25}Ti_{0.25})]O_3$ with frequency at selected temperatures

The large dispersion observed in the $\varepsilon_r \sim$ frequency plot at lower frequency confirms the dominancy of space charge polarization in the material. At all temperature, the value of relative permittivity decreases monotonically as the frequency of perturbed source increases, and all the curves appears to merge at higher frequency suggesting the dielectric nature of

the sample [14]. The larger value of permittivity due to dipolar polarization in the low frequency region is suitable for capacitive and insulating applications of the prepared material. However, at high frequencies, only the ionic polarization exists in the material because it becomes difficult for the dipole moments to respond to the change of field direction and contribute to the dielectric constant. Strong low frequency dispersion in the loss tangent pattern is a result of start of dc conductivity probability due to the oxygen vacancy that exist due to larger concentration of lanthanum [15]. It is observed that the permittivity of the observed material is comparable to that of BFO at all frequencies but with a very low dielectric loss which may be due to decrease in the Fe ion concentration and smaller grain size.

Figure 4(a -b) indicates the temperature effect on the relative permittivity (ε_r) and tangent loss (tanδ) of the studied compound at selected frequencies.

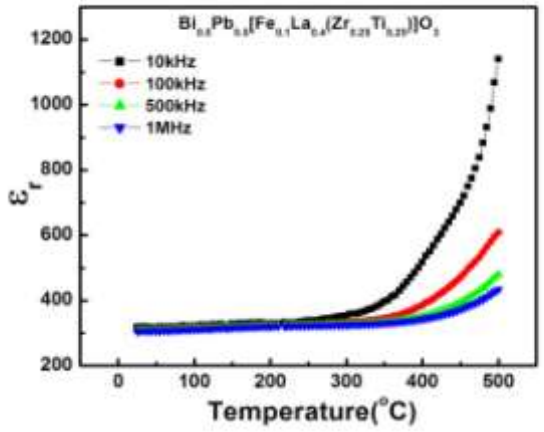

Figure 4(a): Variation of relative dielectric constant (ε_r) of $Bi_{0.5}Pb_{0.5}[Fe_{0.1}La_{0.4}(Zr_{0.25}Ti_{0.25})]O_3$ with temperature at selected Frequencies

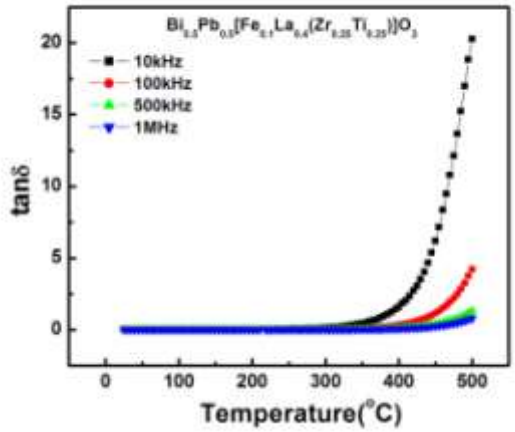

Figure 4(b): Variation of tangent loss ($tan\delta$) of $Bi_{0.5}Pb_{0.5}[Fe_{0.1}La_{0.4}(Zr_{0.25}Ti_{0.25})]O_3$ with temperature at selected frequencies

Generally in ferroelectric materials, the relative permittivity increases with rise in temperature up to the ferroelectric transition temperature and then decreases. The dielectric constant ~ temperature plot of the sample under study shows the same trend as that for a ferroelectric material but the transition is not observed within the experimental temperature range. But the trend of the graph indicates that the substitution on the Bi -site and Fe-sites of BFO lowers the transition temperature. This may be due to lower transition temperature of PZLT [16] as compared to that of BFO. No distinct loss peaks are observed at lower temperature range for any frequency, which may be due to the space charge relaxation phenomena. At higher temperatures free charge carrier conductivity increases in dielectric materials which leads to large dielectric loss [17]. As the concentration of free charge carrier varies with temperature and frequency, the rate of loss decreases at higher frequencies. It may be caused due to the disappearance of space charges at high frequency. However, the lanthanum substitution reduces the lossy effect of the Fe.

3.3 Polarization Study:

Figure- 5 shows the variation of polarization with electric field (P~E loop) at different frequency. The nature of the loops and amount of polarization suggest that addition of elements of PLZT in BFO has significant effect of on the loop's parameters. The existence of polarization suggests the existence of ferroelectricity in the material. The saturation polarization and remnant polarization are found to be 0.48μC/Cm^2, 0.37μC/Cm^2, 0.35μC/Cm^2, 0.33μC/Cm^2 and 0.28μC/Cm^2, 0.12μC/Cm^2, 0.05μC/Cm^2, 0.03μC/Cm^2 at frequencies 1Hz, 2Hz, 5Hz, 10Hz respectively at 50kV/cm. As observed the ferroelectric loss, coercive field, remnant polarization and saturation value of polarization decreases with increase in frequency. Due to experimental limitations on temperature, it was not possible to trace the loop at higher temperatures. Therefore the phase transition (ferroelectric-paraelectric) temperature was not observed with existing experimental facilities as the critical temperature of the $Bi_{0.5}Pb_{0.5}[Fe_{0.1}La_{0.4}(Zr_{0.25}Ti_{0.25})]O_3$ compound is high.

3.4 Impedance Analysis:

Complex impedance spectroscopy provides fundamental information related to distribution parameters of different micro-regions, such as grain, grain boundary and electrode-electrolyte interfaces in a polycrystalline material [18, 19] and also helps to isolate the contributions of bulk, grain boundary and electrode space charge effect towards the ferroelectric behavior and impedance of the material at different frequency domain. This technique helps to correlate the electrical and structural characteristic of the polycrystalline sample at various temperatures in a wide frequency range. The complex impedance of the material can be expressed as:

$$Z^* = |Z|e^{-i\theta} \quad \text{(Cartesian form)}$$

$$= |Z|\cos\theta - i\,|Z|\sin\theta \quad \text{(Polar form)}$$

$= Z' - iZ''$

Where $i = \sqrt{-1}$, $Z' = |Z|\cos\theta$ and $Z'' = |Z|\sin\theta$ are the real and imaginary parts of the complex impedance Z^*respectively.

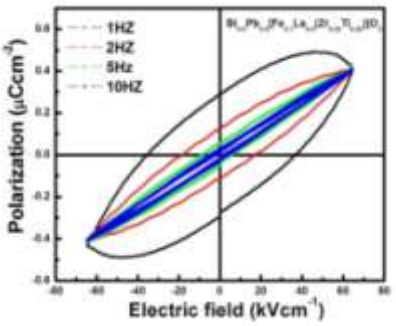

Figure 5: Room temperature hysteresis loop of $Bi_{0.5}Pb_{0.5}$ [$Fe_{0.1}La_{0.4}$ ($Zr_{0.25}Ti_{0.25}$)] O_3 at different frequency

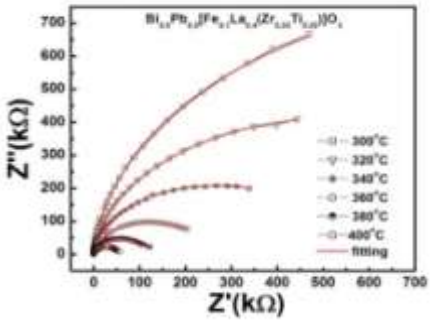

Figure 6: Nyqist plots of $Bi_{0.5}Pb_{0.5}$ [$Fe_{0.1}La_{0.4}$ ($Zr_{0.25}Ti_{0.25}$)] O_3 c at selected high temperature

Figure-6 shows complex impedance spectra of the compound $Bi_{0.5}Pb_{0.5}$ [$Fe_{0.1}La_{0.4}$ ($Zr_{0.25}Ti_{0.25}$)] O_3 at selected high temperatures. The temperature effect on the complex impedance of the sample is remarkable at high temperatures. At high temperature, the complex impedance spectra of the material are characterized by a single semicircular arc which radius of curvature reduces with rise in temperature. Thus bulk resistance reduces with increase in temperature, and hence the ac conductivity of the material increases with temperature. It indicates that the material exhibit NTCR behavior. Even at elevated temperatures, no second semicircular arc is observed, indicating negligible grain boundary effect on overall electrical response of the compound [20, 21]. The transformation of arcs with variation of temperature confirms the occurrence of single relaxation process characterized by a distribution of relaxation times with a mean relaxation time. The incomplete and depressed semicircular arcs observed in the complex impedance plots indicate non- Debye type relaxation process in the material [22,23]. A multiple relaxation process seems to coexist in real perovskite crystals due to various energy barriers, which may be the cause of deviation from ideal Debye like response in the studied sample. An equivalent circuit model is used (given inset) to compare the Nyquist plots (represented by scattered symbols) with fit data (solid line) with the help of a commercially available software ZSimpWin. The values of fit parameters of the compound are presented in Table 1.

Table-1: Comparison of impedance parameters of $Bi_{0.5}Pb_{0.5}$ [$Fe_{0.1}La_{0.4}$ ($Zr_{0.25}Ti_{0.25}$)] O_3 ceramic compound at selected frequencies in high temperature range.

Compound	Temp(^oC)	R_b(Kohm)	C_b(nF)	R_{gb}(Kohm)	C_{gb}(nF)	A	n
$Bi_{0.5}Pb_{0.5}$ [$Fe_{0.1}La_{0.4}$ ($Zr_{0.25}Ti_{0.25}$)] O_3	300	2146	0.1240	1.226	4.324	1.276 x 10^{-7}	0.527
	320	1129	0.1344	4.489	1.129	2.188 x10^{-7}	0.507
	340	706.9	0.1224	3.172	1.017	3.592 x10^{-7}	0.494
	360	296.7	0.1570	2.709	5.574	6.459 x10^{-7}	0.479
	380	116.5	0.1218	14.51	6.017	1.259 x10^{-7}	0.461
	400	60.88	0.1229	2.574	8.343	1.644 x 10^{-6}	0.472

3.5. Ac Conductivity (σ_{ac}):

The transportation of charges in dielectric materials produces conduction current and also polarizes the dielectric [24]. Properties like piezoelectric, pyroelectric, etc of a ferroelectric material depends on its electrical conductivity. The nature of variation of ac conductivity (σ_{ac}) of dielectric materials with temperature and frequency of perturbed electric field suggests the type of charge transportation mechanism in the material. The temperature dependence of σ_{ac} shows that single and multiple relaxation process exists in the material. In polycrystalline materials, conduction mechanisms are of two types;

(i) ac conductivity due to long range hopping of charge carriers and (ii) localized transport of charge carriers due to oxygen vacancies. The conductivity of polar materials is caused by free ions and/or free electrons. conducts e But in polar materials the conduction mechanism can be ionic and/or electronic in nature. The extent of ionic and electronic conduction in a material depends on its purity and temperature. The ac conductivity of the ceramic compound $Bi_{0.5}Pb_{0.5}$ [$Fe_{0.1}La_{0.4}$ ($Zr_{0.25}Ti_{0.25}$)] O_3 was calculated by using following equation;

$$\sigma_{ac} = \omega\epsilon_r\epsilon_o \tan\delta$$

Where, $\epsilon_r\epsilon_o =$ permittivity of the material, tanδ = dielectric loss.

The frequency response of the ac conductivity of the compound at selected high temperatures is shown in Figure 7. The flattened nature of the plots at lower frequencies suggests that the ac conduction in the sample is dominated by the dc conduction. The high-frequency dispersion of conductivity is due to the typical RC network. At higher frequency, the decrease in capacitive reactance of the sample, lowers its impedance, which causes an increase in the ac conductivity of the sample [25-27]. The large slope at higher frequency may be interpreted as the conductivity due to the hopping of the free mobile species.

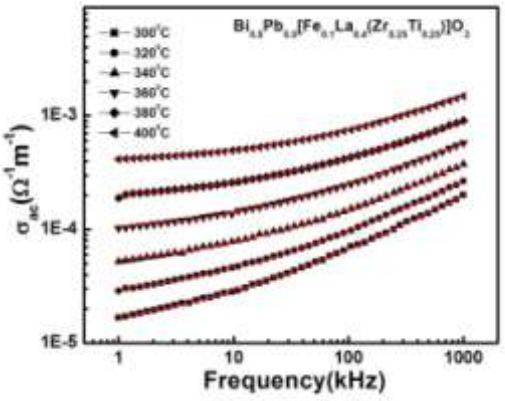

Figure 7: Frequency dependence of ac conductivity of $Bi_{0.5}Pb_{0.5}$ [$Fe_{0.1}La_{0.4}$ ($Zr_{0.25}Ti_{0.25}$)] O_3 at selected high temperature

The hopping increases with increase in frequency (ω) and proportional to ω^n according to Jonscher law : $\sigma_{(\omega)} = \sigma_{dc} + A\omega^n$, which indicates that the response of electrical RC network is qualitatively equivalent to the universal dielectric response(UDR)[28].The factor $A\omega^n$ can be interpreted on the basis of the following two distinct carrier conduction mechanisms:

(i) Charge carrier quantum mechanical tunneling (QMT) between the localized sites through the barrier isolating them.

(ii) Correlated barrier hopping (CBH) of charge carriers

The value of A measures the strength of polarizability in the material. The power of frequency 'n' in Jonscher's equation depends on composition of material and temperature. The value of n ≤ 1, indicates that the motion of charge carriers is translational with a sudden hopping, but the value of n > 1 signifies fumbling of the ionic species in their localized area without leaving their neighborhood [29]. Figure 8(a) and (b) shows the temperature dependence of A and n with for compound $Bi_{0.5}Pb_{0.5}$ [$Fe_{0.1}La_{0.4}$ ($Zr_{0.25}Ti_{0.25}$)]O_3 and their values at selected temperatures were presented in Table-1.

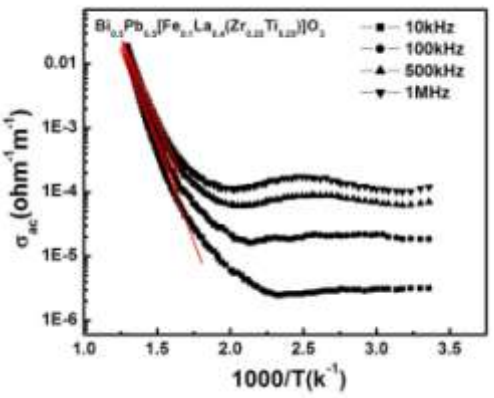

Figure 8 (a): Variation of A with temperature for $Bi_{0.5}Pb_{0.5}$ [$Fe_{0.1}La_{0.4}$ ($Zr_{0.25}Ti_{0.25}$)] O_3 ceramic compound

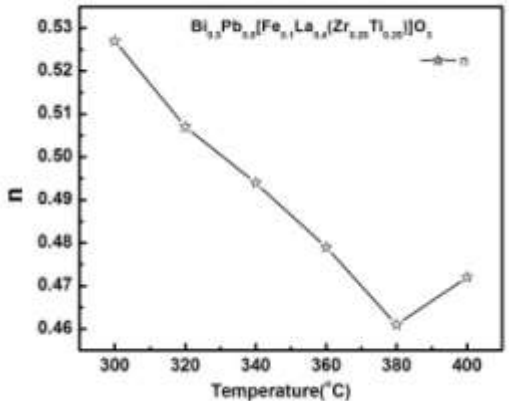

Figure 8(b): Variation of n with temperature for $Bi_{0.5}Pb_{0.5}$ [$Fe_{0.1}La_{0.4}$ ($Zr_{0.25}Ti_{0.25}$)] O_3 ceramic compound

Figure 9 shows the variation of logarithmic value ac conductivity of $Bi_{0.5}Pb_{0.5}$ [$Fe_{0.1}La_{0.4}$ ($Zr_{0.25}Ti_{0.25}$)]O_3 compound with respect to the inverse of absolute temperature (Arrhenius plots) at selected frequencies 10kHz, 100kHz, 500kHz and

1MHz. It is observed that with increase in temperature the ac conductivity of the material increases, which indicates that the material possesses (NTCR) negative temperature coefficient of resistivity. As temperature increases, dispersion in conductivity reduces, and hence all the curves plotted at various frequencies ally to a single curve. It is because of recombination of released space charges at high temperatures [30].The activation energy (E_a) of the sample was found as 1.187eV, 1.184eV, 1.074eV, 1.024eV at frequencies 10^3Hz, 10^5Hz, $5x10^5$Hz, 10^6Hz respectively. The decrease in the activation energy with increase in frequency indicates that smaller energy can overcome the fluctuations caused by the thermal excitation at higher frequencies.

4. CONCLUSION:

The polycrystalline compound $Bi_{0.5}Pb_{0.5}$ [$Fe_{0.1}La_{0.4}$ ($Zr_{0.25}Ti_{0.25}$)] O_3 was prepared by mixed by mixed oxide route. The room temperature XRD data of the sintered powder of the sample indicates that the crystal structure is tetragonal with space group P4mm which is consistent with the previous reports. The scanning electron micrograph of the pellet of the studied sample shows that the grains are distributed uniformly with less porosity. Though the dielectric constant (ε_r) of the sample is observed to be comparable to that of BFO but the dielectric loss decreases drastically in the doped material. Hence, the leakage current in the modified compound is less than that of BFO. The Arrhenius plot of the material indicates that the ac conduction in the material is in accordance with the Jonscher's universal power law. The impedance spectra suggest the existence of non Debye relaxation in the material and the material has negative temperature coefficient of resistivity. Thus the modified compounds have larger potentiality for device applications.

REFERENCES:

1. Lines, M. E. and Glass, A. M. 1977. Principles and Applications of Ferroelectrics and Related Materials. Oxford University Press: New York.
2. Cross, L. E. 1987. Relaxor ferroelectrics, Ferroelectrics: 76, 241-267.
3. Scott, J. F. 2007. Applications of modern ferroelectrics, Science: 315, 954-959.
4. Scott, J. F. 2012. Applications of magnetoelectrics, J. Matter. Chem: 22, 4567.
5. Tejuca, L. G., Ferro, J. L. G., Dekker, Marcel, 1993. Properties and Applications of Perovskite-type oxides.
6. Von Hippel, A. R. 1954. Dielectric lanes and applications, technology, MIT and Wiley press, New York.
7. Panda. N., Pattanayak. S., Choudhary. R.N.P., 2015. Dielectric, impedance and transport characteristics of ($Bi_{0.6}$ $Pb_{0.4}Fe_{0.6}Ti_{0.4}$)O_3.J. Mater. Sci: Materials in Electronics: 26.
8. Ravindran. P., Vidya. R., Kjekshus. A. and Fjellvag. H., 2006. Theoretical investigation of magnetoelectric behavior in $BiFeO_3$, Phy. Rev. B: 74, 224412.
9. Catalan. G. and Scott. J. F., 2009. Physics and Applications of Bismuth Ferrite, Adv. Mater: 21, 2463–2485.
10. Smirnova. E. P., Sotnikov. A., Ktitorov. S., Zaitseva. N., Schmidt. H.and Weihnacht. M., 2011. Acoustic properties of multiferroic BiFeO3 over the temperature range 4.2–830 K, Eur. Phys. J.: B 83, 39.
11. POWDMULT: An interactive Powder Diffraction Data Interpretation and Indexing Program Version 2.1, E.Wu School of Physical Sciences, Flinders University of South Australia, Bradford Park, SA 5042, Australia.
12. Glazer. A. M., 1972. The Classification of Tilted Octahedra in Perovskites, Acta. Cryst. B-28, 3384.
13. Goldschmidt. V. M., 1926. 'Die gesetze der krystallochemie', Naturwissenschafen. 14, 477.
14. Pattanayak. S., Priyadarshan. A., Subudhi. R., 2013. Tailoring of electrical properties of $BiFeO_3$ by praseodymium, J. Adv. Ceram. 2: 3, 235-241.
15. Zhang. S. T. et al, 2008. Substitution- induced phase transition and enhanced multiferroic properties of $Bi_{1-x}La_xFeO_3$ ceramics, Appl. Phys. Lett.:88, 162901.
16. Habouti. S.,Solterbech. C. H. and Es-Souni. 2007. $LaMnO_3$ effects on the ferroelectric and magnetic properties of chemical solution deposited $BiFeO_3$ thin films, M., J. Appl. Phys. 102, 074107.
17. Dutta. S., Choudhary. R. N. P., 2008. Effect of trivalent iron substitution on structure and properties of PLZT ceramics, Appl. Phys. A, 90, 323-328.
18. Bauerle. J. E., 1969. Study of solid electrolyte polarization by a complex admittance method, J. Phys. Chem. Solids. 30, 2657-2670.
19. Park. J.H., Choi. B. C., 2005. Impedance spectroscopy of ($Pb_{0.98}$ $La_{0.02}$)($Zr_{0.95}$ $Ti_{0.05}$)O_3(PLZT-2/95/5) ceramics above ferroelectric phase transition temperatures, J Crystal Growth, 276, 465-470.
20. Laha. A. and Krupanidhi. S. B., 2003. Dielectric response and impedance spectroscopy of $0.7Pb(Mg_{1/3}Nb_{2/3})O_3 – 0.3PbTiO_3$ thin films, Materials Sc. & Engg. B: 98, 204-207.

21. Sen. S., Choudhary. R.N. P., Tarafdar. A., Pramanik. P., 2006. Impedance spectroscopy study of strontium modified lead zirconate titanate ceramics, J. Mater Sci. 99, and 124114-8.

22. Nobre. M. A. L., Lanfredi. S., 1996. Grain boundary electric characterization of $Zn_7Sb_2O_{12}$ semiconducting ceramics : A negative temperature coefficient thermistor, Journal de Physique III: 6, 863-872.

23. Jonscher. A. K., 1980. Non-Debye dielectric tresponses, J. Phy. D: Apll. Phys: 13, L89-93.

24. Bruce. P. G., West. A. R., 1983. The ac conductivity of polycrystalline LISICON, $Li_{2+2x}Zn_{1-x}GeO_4$ and a model for inter-granular constriction resistances, J. Electrochem. Soc. 130, 662-669.

25. Jiang. S. P., Love. J. G., Badwal. S. P. S., 1997. Electrical properties of Oxide materials, Key Engg. Materials: 81, 125-126.

26. Panda.N. Pattanayak.S., Choudhary. R. N. P., 2015. Structural and electric properties of $BiFeO_3$ – $PbTiO_3$ system, J Mater Sci: Mater Electron 26:4069–4077.

27. Venkateswarlua. P., Laha, Krupanidhi. S. B., 2005. AC properties of laser ablated La-modified lead titanate thin films, Thin Solid Films: 474, 1-9.

28. Ngai. K. L., White. C. T., 1979. Frequency dependence of dielectric loss in condensed matter, Phys. Rev. B: 20, 2475-2486.

29. Jonscher. A.K., 1975. The interpretation of non-ideal dielectric admittance and impedance diagrams, Phys. Stat. Solidi (a): 32, 665-676.

30. Jonscher. A. K., 1977. The universal dielectric response, Nature: 267, 673-682.